TITLE

Two parallel pathways convey distinct visual information to the *Drosophila* mushroom body

AUTHOR NAMES AND AFFILIATIONS

Jinzhi Li[1], Brennan Dale Mahoney[1], Miles Solomon Jacob[1] and Sophie Jeanne Cécile Caron[1]

1. School of Biological Sciences, University of Utah, Salt Lake City, Utah 84103

ABSTRACT

The ability to integrate input from different sensory systems is a fundamental property of many brains. Yet, the patterns of neuronal connectivity that underlie such multisensory integration remain poorly characterized. The *Drosophila* mushroom body — an associative center required for the formation of olfactory and visual memories — is an ideal system to investigate how neurons of different sensory channels converge in higher-order brain centers. The neurons connecting the mushroom body to the olfactory system have been described in great detail in *Drosophila melanogaster*, but input from other sensory systems remains poorly defined. Here, we used a range of anatomical and genetic techniques to identify two novel types of mushroom body input neuron that connect a processing center — the lobula— to the dorsal accessory calyx of the mushroom body. Together with previous work showing that the ventral accessory calyx of the mushroom body receives input from another visual processing center, the medulla (Vogt et al., 2016) our results define a second, parallel pathway that conveys visual information to the mushroom body. This connectivity pattern could be a fundamental feature of the neuronal architecture underlying multisensory integration in associative brain centers.

INTRODUCTION

Sensory systems use different strategies to detect specific physical features of the outside world. For instance, the olfactory system contains many different types of sensory neuron that are each specialized in detecting a specific class of volatile chemicals. Through only two neuronal layers, olfactory information — the identity of an odor and its concentration — is relayed to higher brain centers (Leinwand and Chalasani, 2011). In contrast, the visual system contains far fewer types

of sensory neuron but, through numerous neuronal layers, it relays a range of highly processed information — for instance, color, brightness, motion and shape — to higher brain centers (Baden et al., 2020). Thus, higher brain centers have to integrate different types of processed information, bind that information into a coherent representation of the outside world, and use such representations to guide behavior (Yau et al., 2015). How they achieve this remains largely unknown. This gap in our knowledge mainly stems from the fact that higher brain centers are formed by a large number of neurons, and that the projection neurons conveying information from different sensory systems to higher brain centers often remain poorly characterized. This makes it difficult to understand whether there are specific patterns of neuronal connectivity that enable multisensory integration and what these patterns are. Deciphering the fundamental neuronal mechanisms that underlie multisensory integration requires a model system such as the *Drosophila melanogaster* mushroom body, which consists of a relatively small number of neurons whose connections can be charted reliably.

The *Drosophila* mushroom body is formed by ~2,000 neurons — called the Kenyon cells — and has long been studied for its essential role during the formation of olfactory associative memories (Aso et al., 2014; Hige, 2018). The identity of the projection neurons that connect the olfactory system to the mushroom body — and the way Kenyon cells integrate input from these neurons — has been characterized in great detail, highlighting fundamental connectivity patterns that enable this higher brain center to represent olfactory information efficiently (Bates et al., 2020; Caron et al., 2013; Tanaka et al., 2012a, 2012b; Zheng et al., 2018). Evidence in *Drosophila* shows that the mushroom body is more than an olfactory center and that it is also required for the formation of visual and gustatory associative memories (Liu et al., 1999; Masek and Scott, 2010; Vogt et al., 2014). However, the identity of the neurons connecting the mushroom body to other sensory systems remains poorly characterized. Thus, a first step towards understanding how the mushroom body integrates multisensory information is to identify such non-olfactory mushroom body input neurons.

The mushroom body receives its input through its calyx and sends its output through its lobes. The calyx — a morphologically distinct neuropil containing the synapses formed between projection neurons and Kenyon cells — can be divided into four parts: one main calyx as well as three accessory calyces named the dorsal, lateral and ventral accessory calyces (Aso et al., 2014; Yagi et al., 2016). The five output lobes — the α, α', β, β' and γ lobes — contain the synapses formed between Kenyon cells, the mushroom body output neurons and dopaminergic neurons

(Aso et al., 2014). With respect to these input and output regions, Kenyon cells can be divided into seven distinct classes (Aso et al., 2014). Of these seven classes, five classes — the α/β_c, α/β_s, α'/β'_{ap}, α'/β'_m and γ_{main} Kenyon cells — extend their dendrites into the main calyx and their axons along one or two lobes. Most of the neurons projecting to the main calyx emerge from the antennal lobe, the primary olfactory center in the *Drosophila* brain, thus α/β_c, α/β_s, α'/β'_{ap}, α'/β'_m and γ_{main} Kenyon cells receive input primarily from the olfactory system (Aso et al., 2014; Zheng et al., 2018) Here, we refer to these neurons as “olfactory Kenyon cells”.

In addition, two other classes of Kenyon cells do not extend dendrites in the main calyx. Instead, the α/β_p Kenyon cells extend their dendrites into the dorsal accessory calyx and their axons along the α and β lobes, whereas the γ_d Kenyon cells extend their dendrites into the ventral accessory calyx and their axons along the γ lobe (Aso et al., 2014; Vogt et al., 2016). Thus, both the α/β_p and γ_d Kenyon cells are anatomically poised to receive non-olfactory input. There is evidence suggesting that the ventral accessory calyx receives input from the medulla, a region of the optic lobe specialized in processing brightness and color, and that the dorsal accessory calyx might integrate input across sensory systems (Morante and Desplan, 2008; Vogt et al., 2016; Yagi et al., 2016).

Here, we report a strategy that uses a combination of genetic tools — including transgenic lines driving expression in few neurons and a photo-labelling technique used to identify individual neurons and their presynaptic partners — to characterize the input neurons of the α/β_p Kenyon cells. We identify two novel types of mushroom body input neurons that together form about a fifth of the total input the α/β_p Kenyon cells receive. The first type of neuron — henceforth referred to as $_{LO}$PNs — consists of neurons projecting from the lobula, a region of the optic lobe specialized in detecting visual features such as shape and motion. The second type of neuron — henceforth referred to as $_{PLP}$PNs — consists of projection neurons emerging from the posterior lateral protocerebrum, a brain region that also connects to the lobula (Otsuna and Ito, 2006; Keleş and Frye, 2017; Wu et al., 2016). Based on these findings, we conclude that there are two parallel pathways conveying visual information to the mushroom body: a pathway projecting from the medulla to the γ_d Kenyon cells and another pathway projecting from the lobula to the α/β_p Kenyon cells (Vogt et al., 2016).

RESULTS

Neurons projecting to the dorsal accessory calyx emerge from different sensory centers

The dorsal accessory calyx is a neuropil formed from the synapses connecting ~90 α/β_p Kenyon cells to their input neurons (Figure 1; (Aso et al., 2014)). Using transgenic lines driving expression specifically in the α/β_p Kenyon cells (the *R85D07-GAL4$_{DBD}$* and *R13F02-GAL4$_{AD}$* transgenic lines) and a transgenic line driving a photo-activatable form of GFP or PA-GFP (the *UAS-C3PA-GFP* and *UAS-SPA-GFP* transgenic lines, henceforth referred to as *UAS-PA-GFP*), we photo-labelled individual α/β_p Kenyon cells, revealing their entire morphology (Aso et al., 2014; Datta et al., 2008; Ruta et al., 2010). Individual α/β_p Kenyon cells extend on average 5 ± 1 claw-shaped dendritic terminals (*n* = 11) exclusively into the dorsal accessory calyx and project their axons along the α and β lobes (Figure 1A, B, D). The overall morphology of α/β_p Kenyon cells is similar to the morphology of other types of α/β Kenyon cells; for instance, individual α/β_s Kenyon cells extend on average 6 ± 1 claw-shaped dendritic terminals (*n* = 12) exclusively in the main calyx and project their axons along the α and β lobes (Figure 1A, C, E). It is worth noting that the claws formed by α/β_p Kenyon cells are much smaller in diameter (1.8 ± 0.4 μm; *n* = 9 claws) than the claws formed by the α/β_s Kenyon cells (3.0 ± 0.4 μm; *n* = 10 claws; Figure 1B-C). Thus, the α/β_p Kenyon cells resemble α/β_s and α/β_c Kenyon cells but also differ from them in one major way: the dendrites of the α/β_s and α/β_c Kenyon cells innervate exclusively the main calyx — a region known to receive input from the olfactory system — whereas dendrites of the α/β_p Kenyon cells innervate exclusively the dorsal accessory calyx — an uncharacterized part of the mushroom body.

To start identifying the neurons that project to the dorsal accessory calyx and connect to the α/β_p Kenyon cells, we used a targeted photo-labeling technique that was adapted from previously published techniques (Aso et al., 2014; Datta et al., 2008; Ruta et al., 2010). In order to photo-label only the neurons projecting to the dorsal accessory calyx, not the α/β_p Kenyon cells, we used a combination of transgenes that in concert drive the expression of PA-GFP in all neurons except the Kenyon cells (the *N-Synaptobrevin-GAL4*, *MB247-GAL80* and *UAS-PA-GFP* transgenes); Kenyon cells were labeled instead with the red fluorescent protein DsRed (Figure 2). The brains of adult flies carrying all four transgenes were dissected and imaged using two-photon microscopy (Figure 2A-C). Guided by the expression of DsRed, we targeted the dorsal accessory calyx with high-energy light in order to photo-convert PA-GFP specifically in the

neurons projecting to that area (Figure 2C; insert). Upon photo-labeling, the somata of the neurons that express PA-GFP and that project either dendrites or axons into the dorsal accessory calyx were labeled (Figure 2D-E). On average, 72 ± 23 neurons (*n* = 22) were photo-labeled; the somata of these neurons are located in seven distinct clusters distributed across the brain (Figure 2A, D-E). On the anterior side of the brain, we found three clusters: one located near the antennal lobe (cluster AL containing 3 ± 3 neurons), another one located in the optic lobe (cluster OL containing 1 ± 2 neurons) and one located near the anterior ventral lateral protocerebrum (cluster AVLP containing 6 ± 3 neurons) (Figure 2D, F). On the posterior side of the brain, we found four clusters: one located in the superior medial protocerebrum (cluster SMP containing 4 ± 2 neurons), one located in the superior lateral protocerebrum (cluster SLP containing 20 ± 8 neurons), one located in the lateral horn (cluster LH containing 34 ± 12 neurons) and one located in the posterior lateral protocerebrum (cluster PLP containing 3 ± 2 neurons) (Figure 2E-F). Altogether, these results suggest that the dorsal accessory calyx receives input from a diverse and distributed collection of projection neurons that can be divided into seven clusters.

Identification of transgenic lines driving expression in the dorsal accessory calyx input neurons

Although *en masse* photo-labeling of the neurons projecting to the areas within and around the dorsal accessory calyx gives a good approximation of the number of neurons possibly connecting to the α/β_p Kenyon cells, this technique by no means identifies true pre-synaptic partners. Additionally, because the amount of photo-activated PA-GFP within individual neurons varies significantly between trials, and because of the large number of neurons projecting to the dorsal accessory calyx, it is difficult to resolve the morphology of individual neurons. We therefore sought to identify GAL4 transgenic lines that drive expression specifically in these neurons (Figure 3, Table 1). To identify such lines, we carried out an anatomical screen using the FlyLight collection of GAL4 transgenic lines (Jenett et al., 2012). As a first step, we screened through the FlyLight database — an online catalogue that reports the expression patterns of ~7,000 GAL4 driver lines — and selected 266 transgenic lines which highlighted neuronal processes in the dorsal accessory calyx (Figure 3A-C).

In a second step, we specifically labeled neurons projecting to the dorsal accessory calyx using the same technique as described above but with a different combination of transgenes (the *R_line-GAL4*, *UAS-PA-GFP* and *MB247-DsRed* transgenes). As described above, the brains of

adult flies carrying all three transgenes were dissected and imaged using two-photon microscopy (Figure 3D,F). Guided by the expression of DsRed, we targeted the dorsal accessory calyx with high-energy light in order to convert PA-GFP specifically in the neurons projecting to that region (Figure 3D-E). We selected only the lines that showed both a strong photo-labeling signal and clear pre-synaptic terminals near or in the dorsal accessory calyx for further investigation (Table 1). Possible pre-synaptic terminals — usually bouton-shaped — were distinguished from possible post-synaptic terminals — usually mesh-shaped — based on the recovered photo-labeling signal (Figure 3E). Using this screen strategy, we could identify neurons located in all the seven clusters described above, and a total of 12 transgenic lines were selected for further investigation (Table 1).

Finally, we determined whether the neurons identified in our screen are pre-synaptic partners of the α/β_p Kenyon cells. To this end, we used the GFP-reconstitution across synaptic partners (GRASP) technique (Figure 4) (Feinberg et al., 2008; Macpherson et al., 2015). The expression of the syb::spGFP1-10 fragment, which is tagged to an anchor that specifically targets the pre-synaptic membrane, was expressed in the putative input neurons using the different transgenic lines identified in the screen, and the expression of the complementary spGFP11::CD4 fragment was driven in most of the Kenyon cells using the *MB247-LEXA* transgenic line. As previous studies have demonstrated, the reconstitution of GFP molecules, as indicated by the presence of fluorescent GFP speckles, suggests that the neurons expressing the two complementary fragments form functional synapses (Macpherson et al., 2015). We focused our analyses on the dorsal accessory calyx, clearly visible in the red channel, which is innervated specifically by the α/β_p Kenyon cells. We detected a large number of GFP speckles in the dorsal accessory calyx for four of the twelve lines identified in the screen (Figure 4B-E and Table 1). We also detected a small number of GFP speckles in the same region for three other lines (Figure 4F-H and Table 1). Finally, we did not detect any GFP speckles for the remaining five lines identified in the screen (Figure 4I-M and Table 1). Altogether, our screen identified at least four transgenic lines expressed in neurons that connect to the α/β_p Kenyon cells of the dorsal accessory calyx.

The α/β_p Kenyon cells receive input form the optic lobe and the posterior lateral protocerebrum

To characterize further the morphology of the projection neurons connecting to the α/β_p Kenyon cells, we photo-labeled individual neurons using the transgenic lines recovered from our screen.

To this end, the brains of flies carrying the *R_line-GAL4* and *UAS-PA-GFP* transgenes were dissected, photo-labeled, immuno-stained and imaged using confocal microscopy. We first focused our attention on the transgenic lines in which we had found the strongest GRASP signal (Figure 4B-E and Table 1). Single cell photo-labeling using the *R44H11-GAL4* and *R72D07-GAL4* transgenic lines led to the identification of a first type of neuron projecting from the optic lobe to the dorsal accessory calyx (Figure 5). The projection neurons identified in both lines have a similar overall morphology: their somata are located in cluster PLP, a region medial to the optic lobe, they extend their dendrites into the lobula and they project their axons into the superior lateral protocerebrum, forming many axonal boutons in and near the dorsal accessory calyx (Figure 5B-E). Careful inspection of the arbors these neurons extend in the superior lateral protocerebrum shows subtle differences in their branching patterns (Figure 5B-C). Because these neurons clearly extend dendrites in the lobula, we named them $_{LO}PN_1$ (identified using the *R44H11-GAL4* transgenic line) and $_{LO}PN_2$ (identified using the *R72D07-GAL4* transgenic line) (Figure 5D-E). Each neuron innervates a small region of the superior part of the lobula, a center involved in processing visual features such as shape and motion (Figure 5F-G) (Keleş and Frye, 2017; Wu et al., 2016). Thus, the first type of input neuron we identified connects the dorsal accessory calyx to a visual processing center, the lobula.

Similarly, single cell photo-labeling using the *R19H07-GAL4* and *R20G07-GAL4* transgenic lines led to the identification of a second type of neuron projecting from the posterior lateral protocerebrum to the dorsal accessory calyx (Figure 6). The projection neurons identified in both lines have an overall similar morphology: their somata are located near the lateral horn and they extend projections in several brain regions including the posterior lateral protocerebrum, superior lateral protocerebrum, superior clamp and dorsal accessory calyx (Figure 6B-C). Because $_{PLP}$PNs extend projections in the posterior lateral protocerebrum, a poorly characterized brain region processing visual information, we named these neurons $_{PLP}$PNs. We could identify 13 ± 4 $_{PLP}$PNs (n = 21) per hemisphere using the *R19H07-GAL4* transgenic line. The *R20G07-GAL4* transgenic line drives expression at a low level making it difficult to analyze the $_{PLP}$PNs in great detail. To determine whether the $_{PLP}$PNs identified in the *R19H07-GAL4* and *R20G07-GAL4* transgenic lines are the same neurons, we used the split-GAL4 technique (Luan et al., 2006). In this technique, the GAL4 transcription factor is split into two complementary fragments — the $GAL4_{AD}$ and $GAL4_{DBD}$ domains — that are both transcriptionally inactive when expressed alone; when both fragments are expressed in the same cell, GAL4 can be reconstituted and recover its transcriptional activity. $_{PLP}$PNs were visible in flies carrying the *R20G07-GAL4*$_{DBD}$ and *R19H07-*

GAL4$_{AD}$ transgenes thus suggesting that both lines are expressed in the same the group of $_{PLP}$PNs (Figure 6D-G). To distinguish the axonal terminals from the dendritic arbors, we used the split-GAL4 combination of transgenic lines (the *R20G07-GAL4$_{DBD}$* and *R19H07-GAL4$_{AD}$* transgenic lines) to drive the expression of the presynaptic marker synaptotagmin specifically in the $_{PLP}$PNs (Figure 6D). We found that the projections extending into the superior lateral protocerebrum, superior clamp and dorsal accessory calyx contain presynaptic terminals (Figure 6D). Similarly, when the expression of the postsynaptic marker DenMark was driven specifically in the $_{PLP}$PNs, we find that all the projections made by the $_{PLP}$PNs contain postsynaptic terminals (Figure 6E). To investigate further the diversity of neurons among the $_{PLP}$PNs, we used the MultiColor FlpOut (MCFO) approach, a technique that enables multicolor stochastic labeling (Nern et al., 2015). We used the combination of *R20G07-GAL4$_{DBD}$* and *R19H07-GAL4$_{AD}$* transgenic lines to drive the expression of the MCFO transgenes specifically in the $_{PLP}$PNs. We could label between two and five neurons per hemisphere, showing that all $_{PLP}$PNs show overall a similar morphology with minor differences (Figure 6F-G).

Finally, single cell photo-labeling using the transgenic lines that displayed weak GRASP signal — these are the *R30E11-GAL4*, *R31C03-GAL4* and *R53B06-GAL4* lines — led to the identification of a third type of neuron projecting from the posterior antennal lobe to regions around or near the dorsal accessory calyx (data not shown). The projection neurons identified in each line have an overall similar morphology: their somata are located near the antennal lobe, they extend dendrites in the posterior antennal lobe — a region processing hygrosensory and thermosensory information — and axon in several regions including the superior lateral protocerebrum (Table 1). However, unlike the $_{LO}$PNs and $_{PLP}$PNs, each of these neurons extend axonal terminals near but not in the dorsal accessory calyx (data not shown). This might explain why the GRASP signal detected using these transgenic lines was considerably weaker (Figure 4F-H). Likewise, single cell photo-labeling using the transgenic lines that displayed no GRASP signal — these are the *R11F08-GAL4*, *R11F07-GAL4* and *R12C04-GAL4* transgenic lines — revealed neurons projecting dendrites into the anterior or posterior antennal lobe. However, none of these neurons extend axonal terminals in the dorsal accessory calyx (Figure 4I-K). Because all these neurons project from the posterior antennal lobe, we refer to them as $_{PAL}$PNs. Interestingly, a recent study shows that neurons resembling $_{PAL}$PNs are presynaptic to a subset of α'/β'_{ap} Kenyon cells that innervate the lateral accessory calyx (Marin et al., 2020). Altogether, these results show that we could identify two types of neuron — $_{LO}$PNs and $_{PLP}$PNs — that are

presynaptic to the α/β_p Kenyon cells and a third type of neuron — $_{PAL}$PNs — that project close to the dorsal accessory calyx but that are not presynaptic to the α/β_p Kenyon cells.

A fifth of the input of the α/β_p Kenyon cells is to $_{LO}$PNs and $_{PLP}$PNs

A previous study has demonstrated that a technique using a combination of photo-labeling and dye-labeling tools can be used to identify the complement of input individual Kenyon cells receive from the antennal lobe, and the frequency at which individual projection neurons connect to Kenyon cells (Caron et al., 2013). We have modified this technique in order to directly measure the connectivity rate between α/β_p Kenyon cells receive and $_{LO}$PNs and $_{PLP}$PNs. In this modified version of the technique, we use a combination of transgenic lines such that we can photo-label the projection neuron of interest and dye-label an α/β_p Kenyon cell. We can then assess how many of the dendritic claws formed by the dye-labeled Kenyon cell are connected to a given projection neuron. As a proof of principle, we measured the connectivity rate of the DC3 glomerulus projection neurons to Kenyon cells innervating the main calyx, which has been previously approximated to be 5.1% (Caron et al., 2013). Using the modified technique, we found that the DC3 projection neurons connect to Kenyon cells at a connectivity rate of 4.3% (n = 30), a value well within the range measured previously (data not shown). We measured the connectivity rates to the α/β_p Kenyon cells for most of the projection neurons identified in our screen (Figure 7). We found that of 4.1 % (n = 27) of the α/β_p Kenyon cells input is from $_{LO}$PN1 (Figure 7B-C and Table 1). Likewise, we found that of 3 % (n = 27) of the α/β_p Kenyon cells input is from $_{LO}$PN2 (Table 1). By far, the highest connectivity rate was obtained for $_{PLP}$PNs, which constitute of 14.1 % (n = 24) of the α/β_p Kenyon cell input, with each $_{PLP}$PN connecting on average at a frequency rate of 1.9 % (n = 32) (Figure 7D-E and Table 1). We also measured the connectivity rates for all the $_{PAL}$PNs. As expected, we failed to detect any connections between the α/β_p Kenyon cells and $_{PAL}$PN1 (identified using the *R30E11-GAL4* and *R31C03-GAL4* transgenic lines), $_{PAL}$PN2 (identified using the *R53B06-GAL4* transgenic line), $_{PAL}$PN3 (identified using the *R11F08-GAL4* and *R12C04-GAL4* transgenic lines) and $_{PAL}$PN4 (identified using the *R11F07-GAL4* transgenic line) (Figure 7F-H and Table 1). Altogether, these results confirm that $_{LO}$PNs and $_{PLP}$PNs are true presynaptic partners of the α/β_p Kenyon cells and that together these two types of projection neuron represent about a fifth of the total input α/β_p Kenyon cells receive.

DISCUSSION

In this study, we have identified and characterized neurons projecting to the dorsal accessory calyx of the mushroom body and show that these neurons are presynaptic to the α/β_p Kenyon cells (Figure 8). Using a combination of genetic and anatomical techniques, we could distinguish two different types of projection neuron: the $_{LO}$PNs projecting from the lobula — an area of the optic lobe processing visual features such as shape and motion — and the $_{PLP}$PNs projecting from the posterior lateral protocerebrum. Although the posterior lateral protocerebrum remains poorly characterized in *Drosophila*, evidence from other insects shows that this brain region receives input from the lobula and processes visual features such as motion and shape (Paulk et al., 2008, 2009). Altogether, we estimate that $_{LO}$PNs and $_{PLP}$PNs account for a fifth of the total input of α/β_p Kenyon cells. $_{LO}$PNs and $_{PLP}$PNs do not extend axonal terminals into the ventral accessory calyx, the other calyx known to receive visual input, but rather extend axonal terminals into the dorsal accessory calyx and into the superior lateral protocerebrum. Likewise, the α/β_p Kenyon cells do not connect to the visual projection neurons associated with the ventral accessory calyx (Vogt et al., 2016). These findings suggest that the visual system is connected to the mushroom body via two parallel pathways: the α/β_p Kenyon cells receive input from the lobula and the posterior lateral protocerebrum, whereas the γ_d Kenyon cells receive input from the medulla.

Our screen did not identify the full complement of input neurons associated with the dorsal accessory calyx and the identity of these neurons remains unclear. Based on the neurons identified by *en masse* photo-labeling of the dorsal accessory calyx, we can predict where the remaining input neurons might be located (Figure 2). For instance, we identified 34 ± 12 neurons in the LH cluster — the largest cluster that contains the $_{PLP}$PNs — but the transgenic lines identified in our screen drive expression in only 13 ± 4 $_{PLP}$PNs (n = 21). Thus, it is possible that there are more $_{PLP}$PNs connecting to α/β_p Kenyon cells. Likewise, our screen could identify a few transgenic lines driving expression in neurons associated with the SLP cluster — the second largest cluster which contains 20 ± 8 neurons — but none of these neurons clearly extend axonal terminals in the dorsal accessory calyx; it is possible that there are $_{SLP}$PNs connecting to α/β_p Kenyon cells. We can, however, rule out that the remaining input neurons belong to the AL cluster: neurons from the AL cluster — which contains the $_{PAL}$PNs that innervate the antennal lobe — did not show positive GRASP signal and most likely do not connect to the α/β_p Kenyon cells. This finding contrasts with a previous study that has identified neurons similar to $_{PAL}$PNs as dorsal

accessory calyx input neurons (Yagi et al., 2016). We tested this further using the GRASP technique and the $_{PAL}$PNs specific transgenic line identified in this study (*R64G05-GAL4*), but could not detect a positive GRASP signal (Figure 4L). Similarly, we could identify a transgenic line, *R21B02-GAL4*, driving expression in a neuron associated with the OL cluster — which contains 1 ± 2 neurons — projecting from the medulla. However, we could not detect a positive GRASP signal using this transgenic line (Figure 4M). We do not expect neurons within the other clusters that contain only a few neurons — clusters AVLP, PLP and SMP — to be major input neurons of the dorsal accessory calyx. Although our study did not provide the full set of dorsal accessory calyx input neurons, these neurons are now identifiable using the connectome of a fly brain hemisphere (Xu et al., 2020). Keeping this in mind, our data set — because it identifies transgenic lines that drive expression in many neurons associated with the dorsal accessory calyx — will be instrumental in developing the tools required to manipulate and further analyze the dorsal accessory calyx input neurons.

In *Drosophila melanogaster*, the mushroom body has long been studied as an olfactory processing center. However, evidence from many insects, including the honeybee *Apis mellifera*, shows that the mushroom body integrates sensory information across different modalities. In honeybees, the input region of the mushroom body, also called the calyx, is divided into different layers and each layer receives input from either the olfactory or visual system (Gronenberg, 2001). Because the dendrites of Kenyon cells are also restricted to specific layers, it has been suggested that in the honeybee multisensory integration does not occur at the level of individual Kenyon cells, but rather at the population level (Ehmer and Gronenberg, 2002). Although the honeybee mushroom body differs greatly from the *Drosophila* mushroom body — it contains about a hundred times as many Kenyon cells and its input region is divided in multiple complex layers — it appears that both mushroom bodies share a common fundamental connectivity principle: the segregation of input based on sensory modality. This connectivity mechanism is immediately apparent in the structural organization of the *Drosophila melanogaster* mushroom body: the Kenyon cells receiving input from the olfactory system all extend their dendrites in the main calyx, whereas as the Kenyon cells receiving input from the visual system extend their dendrites either in the dorsal accessory calyx or the ventral calyx. Many studies have demonstrated that the Kenyon cells processing olfactory information — those associated with the main calyx — integrate input broadly across the different types of olfactory projection neuron (Caron et al., 2013; Zheng et al., 2018). Interestingly, it appears that the Kenyon cells processing visual information are wired differently.

In *Drosophila melanogaster*, we understand very well how olfactory Kenyon cells integrate input from the antennal lobe: most Kenyon cells receive, on average, input from seven projection neurons and the projection neurons connecting to the same Kenyon cell share no common features (Caron et al., 2013; Zheng et al., 2018). Theoretical studies have shown that this random-like connectivity pattern enables the mushroom body to form sparse and decorrelated odor representations and thus maximizes learning (Litwin-Kumar et al., 2017). Randomization of sensory input is a connectivity pattern well suited for representing olfactory information — as an odor is encoded based on the ensemble of olfactory receptors it activates — and might not be suitable for representing visual information. Indeed, our results suggest that that specific visual features — the signals processed by the medulla and the one processed by the lobula — need to be represented by separate subpopulations of Kenyon cells. This mirrors anatomical studies of the honeybee brain: the neurons projecting from the lobula terminate in a different layer than the neurons projecting from the medulla (Ehmer and Gronenberg, 2002). This arrangement might be essential to preserve distinct visual features when forming associative memories. Further anatomical and functional studies are required to determine whether indeed the mushroom body represents multisensory stimuli this way.

MATERIAL AND METHODS

Fly stocks

Flies (*Drosophila melanogaster*) were raised on standard cornmeal agar medium and maintained in an incubator set at 25°C, 60% humidity with a 12 hours light / 12 hours dark cycle (Percival Scientific, Inc.). Crosses were set up and reared in the same conditions, but the standard cornmeal agar medium was supplemented with dry yeast. The strains used in this study are described in the table below.

Transgene(s)	Bloomington number	FlyLight number	Reference
GAL4 transgenic lines:			
yw;N-Synaptobrevin-GAL4$^{2.1}$;;	N/A	N/A	Aso *et al.*
y^{1}w^{1118};;R11F07-GAL4^{attP2};	39414	R11F07	Jenett *et al.*
y^{1}w^{1118};;R11F08-GAL4^{attP2};	48467	R11F08	Jenett *et al.*
y^{1}w^{1118};;R12C04-GAL4^{attP2};	48494	R12C04	Jenett *et al.*

y^{1}*w*^{1118}*;;R19H07-GAL4*^{attP2};	48867	R19H07	Jenett *et al.*
y^{1}*w*^{1118}*;;R20G07-GAL4*^{attP2};	48613	R20G07	Jenett *et al.*
y^{1}*w*^{1118}*;;R30E11-GAL4*^{attP2};	48100	R30E11	Jenett *et al.*
y^{1}*w*^{1118}*;;R21B02-GAL4*^{attP2};	49293	R21B02	Jenett *et al.*
y^{1}*w*^{1118}*;;R31C03-GAL4*^{attP2};	48103	R31C03	Jenett *et al.*
y^{1}*w*^{1118}*;;R53B06-GAL4*^{attP2};	38863	R53B06	Jenett *et al.*
y^{1}*w*^{1118}*;;R44H11-GAL4*^{attP2};	41268	R44H11	Jenett *et al.*
y^{1}*w*^{1118}*;;R64G05-GAL4*^{attP2};	39316	R64G05	Jenett *et al.*
y^{1}*w*^{1118}*;;R72D07-GAL4*^{attP2};	39770	R72D07	Jenett *et al.*
Split-GAL4 transgenic lines:			
y^{1}*w*^{1118}*;;R13F02-GAL4*$_{AD}$^{VK00027}*,R85D07-GAL4*$_{DBD}$^{attP2};	N/A	R_MB371C	Aso *et al.*
y^{1}*w*^{1118}*;R52H09-GAL4*$_{AD}$^{attP40}*;R18F09-GAL4*$_{DBD}$^{attP2};	68267	R_MB185B	Aso *et al.*
y^{1}*w*^{1118}*;R19H07-GAL4*$_{AD}$^{attP40}*;R20G07-GAL4*$_{DBD}$^{attP2};	N/A	N/A	this study
UAS transgenic lines:			
yw;UAS-C3PA-GFP^{unknown}*;;*	N/A	N/A	Ruta *et al.*
y^{1}*w*^{1118}*;UAS-C3PA-GFP*^{attP40}*;;*	N/A	N/A	Aso *et al.*
y^{1}*w*^{1118}*;;UAS-C3PA-GFP*^{attP2};	N/A	N/A	Aso *et al.*
y^{1}*w*^{1118}*;;UAS-C3PA-GFP*^{VK00005};	N/A	N/A	Aso *et al.*
y^{1}*w*^{1118}*;UAS-SPA-GFP*^{attP40}*;;*	N/A	N/A	Aso *et al.*
yw;UAS-syb::spGFP1-10^{unknown}*;;*	N/A	N/A	Macpherson *et al.*
yw;UAS-DenMark^{2}*;;*	33062	N/A	Nicolaï *et al.*
yw;; UAS-synaptotagmin::GFP^{3};	6926	N/A	Nicolaï *et al.*
y^{1}*w*^{1118}*;;UAS-FRT>STOP>FRT-myr::smGdP-HA*^{VK00005}*,UAS-FRT>STOP>FRT-myr::smGdP-V5-THS,UAS-FRT>STOP>FRT-myr::smGdP-FLAG*$^{su(Hw)attP1}$*;*	64085	MCFO1	Nern *et al.*
GAL80 transgenic lines:			
yw;MB247-GAL80^{unknown}*;;*	64306	N/A	Krashes *et al.*
LEXA transgenic lines:			
*yw;;*MB247*-LEXA::VP16*^{unknown};	N/A	N/A	Pitman *et al.*
LEXAop transgenic lines:			
yw;LEXAop-CD4::spGFP11^{unknown}*;;*	N/A	N/A	Macpherson *et al.*
yw;LEXAop-tdTomato$^{Su(Hw)attP5}$*;;*	56142	N/A	Chen *et al.*
Direct fusion transgenic lines:			
yw;MB247-DsRed^{unknown}*;;*	N/A	N/A	Riemensperger *et al.*

Photo-labeling neurons using PA-GFP

Two to six day-old flies were used for all photo-labeling experiments. The protocol was largely based on the one developed in a previous study (Aso et al., 2014). In short, brains were dissected in saline (108 mM NaCl, 5 mM KCl, 5 mM HEPES, 5 mM Trehalose, 10 mM Sucrose, 1 mM NaH_2PO_4, 4 mM $NaHCO_3$, 2 mM $CaCl_2$, 4 mM $MgCl_2$, pH≈7.3), treated for 1 minute with 2 mg/ml collagenase (Sigma-Aldrich) and mounted on a piece of Sylgard placed at the bottom of a Petri dish. Photo-labeling and image acquisition were performed using an Ultima two-photon laser scanning microscope (Bruker) with an ultrafast Chameleon Ti:S laser (Coherent) modulated by Pockels Cells (Conotopics). For photo-labeling, the laser was tuned to 710 nm with an intensity of 5-30 mW; for image acquisition, the laser was tuned to 925 nm with an intensity of 1-14 mW (both power values were measured behind the objective lens). A 60X water-immersion objective lens (Olympus) was used for both photo-labeling and image acquisition. A 40X water-immersion objective lens (Olympus) was used for image acquisition in some experiments (the ones described in Figure 2 and Figure 3). A GaAsP detector (Hamamatsu Photonics) and PMT detector were used for measuring green and red fluorescence, respectively. Photo-labeling and image acquisition files were visualized on a computer using the Prairie View software version 5.4 (Bruker). Image acquisition was performed at a resolution of 512 by 512 pixels, with a pixel size of 0.39 µm (60X lens) or 0.582 µm (40X) and a pixel dwell time of 4 µs. Each pixel was scanned 8 times.

For photo-labeling of the dorsal accessory calyx, a volume spanning the entire neuropil was divided into eight to 12 planes with a step size of 2 µm. The mask function of the Prairie View software was used to mark the targeted region in every plane, and the boundaries of the mask were determined based on the red fluorescent protein DsRed expressed by the α/β_p Kenyon cells. The photo-labeling step was performed using a pixel size of 0.019 µm and a pixel dwell time of 2 µs. Each pixel was scanned four times. Each plane was scanned 30 times with 30-second interval. The entire photo-labeling cycle was repeated two to three times, with a 10-minute resting period between cycles. The entire brain was imaged before and after photo-labeling using the 40X water-immersion objective lens (Olympus, Japan). The number of cell bodies recovered after the photo-labeling was measured using the Multi-Point Tool function of the Fiji software (http://fiji.sc/) (Schindelin et al., 2012).

For the photo-labeling of single neurons, a slightly modified protocol was used. Instead of a volume, a single square plane of 1.0 µm by 1.0 µm centered on the soma of a neuron cell was scanned 70 to 100 times with a 10 seconds interval between scans. Photo-labeled brains were first fixed in 2% paraformaldehyde diluted in 1X phosphate bovine saline (PFA) for 45 minutes at room temperature, then washed five times in 0.3% Triton X-100 diluted in 1X phosphate bovine saline (PBST) at room temperature, then blocked in 5% normal goat serum diluted in PBST (PBST-NGS) for 30 minutes at room temperature, and finally incubated with the primary mouse antibody anti-nc82 (1:20 in PBST-NGS; Developmental Studies Hybridoma Bank, University of Iowa) at 4°C overnight. On the following day, brains were washed four times in PBST and incubated with the secondary goat antibody Alexa Fluor 633 anti-mouse (1:500 in PBST-NGS; Life Technologies) at 4°C overnight. On the following day, brains were washed four times in PBST and mounted on a slide (Fisher Scientific) using the mounting media VECTASHIELD (Vector Laboratories Inc.). Immuno-stained brains were imaged using an LSM 880 confocal microscope. (Zeiss). The neuropils innervated by the input neurons were identified by comparing the confocal images with the adult brain template JFRC2 available on Virtual Fly Brain (https://v2.virtualflybrain.org/).

Immunohistochemistry

For the experiments using the green fluorescent protein reconstitution across synaptic partners (GRASP) technique as well as the experiments using DenMark and synaptotagmin::GFP immunostainings, the brains of 5 to 14 day-old flies were dissected in saline and fixed in PFA for 45 minutes at room temperature, then washed five times in PBST at room temperature, then blocked in PBST-NGS for 30 minutes at room temperature, and finally incubated with the primary antibody at 4°C overnight. The mouse anti-GFP-20 antibody was used in GRASP and synaptotagmin experiments (1:100 in PBST-NGS; Sigma-Aldrich); the mouse anti-nc82 antibody was used in synaptotagmin::GFP and DenMark experiments. On the following day, brains were washed four times in PBST and incubated in secondary antibody at 4°C overnight. The AlexaFluor-488 goat-anti-mouse (1:500 in PBST-NGS; Life Technologies) and AlexaFluor-633 goat-anti-mouse (1:500 in PBST-NGS; Life Technologies) were used. On the following day, brains were washed four times in PBST and mounted on a slide (Fisher Scientific) using the mounting media VECTASHIELD (Vector Laboratories Inc.). Immuno-stained brains were imaged using an LSM 880 confocal microscope. (Zeiss). The neuropils innervated by the input neurons were

identified by comparing the confocal images with the adult brain template JFRC2 available on Virtual Fly Brain (https://v2.virtualflybrain.org/) (Jenett et al., 2012).

The protocol used for the MultiColor FlpOut (MCFO) technique was largely based on the one developed by a previous study (Nern et al., 2015). In short, two day-old flies were placed in vials with standard cornmeal agar medium and incubated at 37°C in a water bath for one hour, in order to induce the expression of the recombinase flippase. Brains were dissected in saline at least two days after the heat-shock treatment, fixed in PFA for 55 minutes at room temperature, washed four times in PBST at room temperature, blocked in PBST-NGS for 90 minutes at room temperature and incubated with the primary antibodies, first for 4 hours at room temperature, and then for 12 hours at 4°C. The following primary antibodies were used: rabbit anti-HA (1:300; Cell Signaling Technology), rat anti-FLAG (1:200; Novus Biologicals), mouse anti-V5 (1:500, Bio-Rad Laboratories). On the following day, brains were washed three times in PBST and incubated with the secondary antibodies, first for four hours at room temperature, and then for 12 to 36 hours at 4°C. The following secondary antibodies were used: AlexaFluor-488 goat-anti-mouse (1:400; Life Technologies), AlexaFluor-594 donkey-anti-rabbit (1:500; Jackson ImmunoResearch Laboratories) and AlexaFluor-647 donkey-anti-rat (1:150; Jackson ImmunoResearch Laboratories). On the following day, brains were washed three times in PBST and mounted on a slide (Fisher Scientific) using the mounting media VECTASHIELD (Vector Laboratories Inc.). Immuno-stained brains were imaged using an LSM 880 confocal microscope (Zeiss).

Measuring the connectivity rate between input neurons and α/β$_p$ Kenyon cells

One to three day-old flies were used when mapping the connectivity rate between input neurons and α/β$_p$ Kenyon cells. Brains were dissected in saline, treated for one minute with 2 mg/ml collagenase (Sigma-Aldrich) and mounted on a piece of Sylgard placed at the bottom of a Petri dish. The imaging protocol is the same as described above but the photo-labeling protocol is different. Each of the input neurons was photo-labeled using a single plane centered on the soma of a neuron or one of its track cell by scanning the plane three to five times. Each pixel was scanned 8 times with a pixel size of 0.019 µm and a pixel dwell time of 4 µs. A fire-polished borosilicate glass pipette (0.5 mm I.D., 1.0 mm O.D., 10 cm length; Sutter Instruments) was pulled using the P-2000 micropipette puller (Sutter Instruments) and backfilled with Texas Red dye (lysine-fixable 3000 MW; Life Technologies) dissolved in saline. The tip of the pipette was positioned next to the cell body of a randomly chosen α/β$_p$ Kenyon cell under the two-photon microscope. The dye was electroporated

into the cell body using three to five 1-5 millisecond pulses of 20-50 V. The dye was allowed to diffuse within the Kenyon cell for 5 minutes before the brain was imaged.

Confocal image acquisition and analysis

All confocal images were collected on LSM880 confocal microscope (Zeiss). For imaging whole brain, each sample was imaged twice using a Plan-Apochromat 40X/1.3 Oil M27 objective lens. First, the entire brain was divided into four tiles, each tile was imaged separately (voxel size = 0.46 µm by 0.46 µm by 2 µm, 764 by 764 pixels per image plane) and then stitched together using the Stitch function of the Zen microscope software (Zeiss). For imaging specific neuropil regions, the same objective lens was used, but with higher resolution (voxel size = 0.09 µm by 0.09 µm by 1 µm, 2320 by 2320 pixels per image plane). For imaging brains manipulated using the GRASP technique, a Plan-Apochromat 63X/1.4 Oil M27 objective lens was used in combination with the RGB Airyscan mode. Images were processed using the Airyscan processing function of the Zen microscope software. All confocal images were analyzed using the Fiji software (http://fiji.sc/) (Schindelin et al., 2012). All figure panels are maximum intensity projection of confocal stacks or sub-stacks.

AKNOWLEDGMENTS

We thank Florian Maderspacher and members of the Caron laboratory for comments on the manuscript; Shannon Torstrom for the initial characterization of the *y*^{1}*w*^{1118};;*R19H07-GAL4*$_{AD}$^{VK00027};*R20G07-GAL4*$_{DBD}$^{attP2}; transgenic line; Adam Lin for preparation of the standard cornmeal agar medium; Hayley Smihula and Adam Weinbrom for assistance with general laboratory concerns. This work has been funded in part by grants from the National Institute for Neurological Disorders and Stroke (R01 NS 106018 and R01 NS 1079790). Further financial support was provided by the Georges S. and Dolores Eccles Foundation (SJCC), the Dale A. Stringfellow Fellowship (JL), and the Research Scholar Award (MSJ).

COMPETING INTERESTS

The authors declare that no competing interests exist.

REFERENCES

Aso Y, Hattori D, Yu Y, Johnston RM, Iyer NA, Ngo TTB, Dionne H, Abbott LF, Axel R, Tanimoto H, Rubin GM. 2014. The neuronal architecture of the mushroom body provides a logic for associative learning. *eLife* **3**:e04577. doi:10.7554/eLife.04577

Baden T, Euler T, Berens P. 2020. Understanding the retinal basis of vision across species. *Nature Reviews Neuroscience* **21**:5–20. doi:10.1038/s41583-019-0242-1

Bates AS, Schlegel P, Roberts RJ v., Drummond N, Tamimi IFM, Turnbull RG, Zhao X, Marin EC, Popovici PD, Dhawan S, Jamasb AR, Javier A, Li F, Rubin GM, Waddell S, Bock DD, Costa M, Jefferis GSXE. 2020. Complete connectomic reconstruction of olfactory projection neurons in the fly brain. *bioRxiv* 2020.01.19.911453. doi:10.1101/2020.01.19.911453

Caron SJC, Ruta V, Abbott LF, Axel R. 2013. Random convergence of olfactory inputs in the Drosophila mushroom body. *Nature* **497**:113–117. doi:10.1038/nature12063

Datta SR, Vasconcelos ML, Ruta V, Luo S, Wong A, Demir E, Flores J, Balonze K, Dickson BJ, Axel R. 2008. The Drosophila pheromone cVA activates a sexually dimorphic neural circuit. *Nature* **452**:473–477. doi:10.1038/nature06808

Ehmer B, Gronenberg W. 2002. Segregation of visual input to the mushroom bodies in the honeybee (Apis mellifera). *Journal of Comparative Neurology* **451**:362–373. doi:10.1002/cne.10355

Feinberg EH, VanHoven MK, Bendesky A, Wang G, Fetter RD, Shen K, Bargmann CI. 2008. GFP Reconstitution Across Synaptic Partners (GRASP) Defines Cell Contacts and Synapses in Living Nervous Systems. *Neuron* **57**:353–363. doi:10.1016/j.neuron.2007.11.030

Gronenberg W. 2001. Subdivisions of hymenopteran mushroom body calyces by their afferent supply. *Journal of Comparative Neurology* **435**:474–489. doi:10.1002/cne.1045

Hideo Otsuna KI. 2006. Systematic analysis of the visual projection neurons of Drosophila melanogaster: Lobula-specific pathways. *Journal of Comparative Neurology* **497**:928–958.

Hige T. 2018. What can tiny mushrooms in fruit flies tell us about learning and memory? *Neuroscience Research* **129**:8–16. doi:10.1016/j.neures.2017.05.002

Jenett A, Rubin GM, Ngo TTB, Shepherd D, Murphy C, Dionne H, Pfeiffer BD, Cavallaro A, Hall D, Jeter J, Iyer N, Fetter D, Hausenfluck JH, Peng H, Trautman ET, Svirskas RR, Myers EW, Iwinski ZR, Aso Y, DePasquale GM, Enos A, Hulamm P, Lam SCB, Li HH, Laverty TR, Long F, Qu L, Murphy SD, Rokicki K, Safford T, Shaw K, Simpson JH, Sowell A, Tae S, Yu Y, Zugates CT. 2012. A GAL4-Driver Line Resource for Drosophila Neurobiology. *Cell Reports* **2**:991–1001. doi:10.1016/j.celrep.2012.09.011

Keleş MF, Frye MA. 2017. Object-Detecting Neurons in Drosophila. *Current Biology* **27**:680–687. doi:10.1016/j.cub.2017.01.012

Leinwand SG, Chalasani SH. 2011. Olfactory networks: From sensation to perception. *Current Opinion in Genetics and Development* **21**:806–811. doi:10.1016/j.gde.2011.07.006

Litwin-Kumar A, Harris KD, Axel R, Sompolinsky H, Abbott LF. 2017. Optimal Degrees of Synaptic Connectivity. *Neuron* **93**:1153-1164.e7. doi:10.1016/j.neuron.2017.01.030

Liu L, Wolf R, Ernst R, Heisenberg M. 1999. Context generalization in Drosophila visual learning requires the mushroom bodies. *Nature* **400**:753–756. doi:10.1038/23456

Luan H, Peabody NC, Vinson CR, White BH. 2006. Refined Spatial Manipulation of Neuronal Function by Combinatorial Restriction of Transgene Expression. *Neuron* **52**:425–436. doi:10.1016/j.neuron.2006.08.028

Macpherson LJ, Zaharieva EE, Kearney PJ, Alpert MH, Lin TY, Turan Z, Lee CH, Gallio M. 2015. Dynamic labelling of neural connections in multiple colours by trans-synaptic fluorescence complementation. *Nature Communications* **6**:1–9. doi:10.1038/ncomms10024

Marin EC, Roberts RJ v, Büld L, Theiss M, Pleijzier MW, Sarkissian T, Laursen WJ, Turnbull R, Schlegel P, Alexander S, Li F, Landgraf M, Costa M, Bock DD, Garrity PA. 2020. Connectomics analysis reveals first, second, and third order thermosensory and hygrosensory neurons in the adult Drosophila brain.

Masek P, Scott K. 2010. Limited taste discrimination in Drosophila. *Proceedings of the National Academy of Sciences* **107**:14833–14838. doi:10.1073/pnas.1009318107

Morante J, Desplan C. 2008. The Color-Vision Circuit in the Medulla of Drosophila. *Current Biology* **18**:553–565. doi:10.1016/j.cub.2008.02.075

Nern A, Pfeiffer BD, Rubin GM. 2015. Optimized tools for multicolor stochastic labeling reveal diverse stereotyped cell arrangements in the fly visual system. *Proceedings of the National Academy of Sciences* **112**:E2967–E2976. doi:10.1073/pnas.1506763112

Paulk AC, Dacks AM, Phillips-Portillo J, Fellous JM, Gronenberg W. 2009. Visual processing in the central bee brain. *Journal of Neuroscience* **29**:9987–9999. doi:10.1523/JNEUROSCI.1325-09.2009

Paulk AC, Phillips-Portillo J, Dacks AM, Fellous JM, Gronenberg W. 2008. The processing of color, motion, and stimulus timing are anatomically segregated in the bumblebee brain. *Journal of Neuroscience* **28**:6319–6332. doi:10.1523/JNEUROSCI.1196-08.2008

Ruta V, Datta SR, Vasconcelos ML, Freeland J, Looger LL, Axel R. 2010. A dimorphic pheromone circuit in Drosophila from sensory input to descending output. *Nature* **468**:686–690. doi:10.1038/nature09554

Schindelin J, Arganda-Carreras I, Frise E, Kaynig V, Longair M, Pietzsch T, Preibisch S, Rueden C, Saalfeld S, Schmid B, Tinevez JY, White DJ, Hartenstein V, Eliceiri K, Tomancak P, Cardona A. 2012. Fiji: An open-source platform for biological-image analysis. *Nature Methods* **9**:676–682. doi:10.1038/nmeth.2019

Tanaka NK, Endo K, Ito K. 2012a. Organization of antennal lobe-associated neurons in adult Drosophila melanogaster brain. *Journal of Comparative Neurology* **520**:4067–4130. doi:10.1002/cne.23142

Tanaka NK, Suzuki E, Dye L, Ejima A, Stopfer M. 2012b. Dye fills reveal additional olfactory tracts in the protocerebrum of wild-type Drosophila. *Journal of Comparative Neurology* **520**:4131–4140. doi:10.1002/cne.23149

Vogt K, Aso Y, Hige T, Knapek S, Ichinose T, Friedrich AB, Turner GC, Rubin GM, Tanimoto H. 2016. Direct neural pathways convey distinct visual information to drosophila mushroom bodies. *eLife* **5**:1–13. doi:10.7554/eLife.14009

Vogt K, Schnaitmann C, Dylla K v., Knapek S, Aso Y, Rubin GM, Tanimoto H. 2014. Shared mushroom body circuits underlie visual and olfactory memories in Drosophila. *eLife* **3**:e02395. doi:10.7554/eLife.02395

Wu M, Nern A, Ryan Williamson W, Morimoto MM, Reiser MB, Card GM, Rubin GM. 2016. Visual projection neurons in the Drosophila lobula link feature detection to distinct behavioral programs. *eLife* **5**. doi:10.7554/eLife.21022

Xu CS, Januszewski M, Lu Z, Takemura Shin-ya, Hayworth K, Huang G, Shinomiya K, Maitin-Shepard J, Ackerman D, Berg S, Blakely T, Bogovic J, Clements J, Dolafi T, Hubbard P, Kainmueller D, Katz W, Kawase T, Khairy K, Leavitt L, Li PH, Lindsey L, Neubarth N, Olbris DJ, Otsuna H, Troutman ET, Umayam L, Zhao T, Ito M, Goldammer J, Wolff T, Svirskas R, Schlegel P, Neace ER, Knecht CJ, Alvarado CX, Bailey D, Ballinger S, Borycz JA, Canino B, Cheatham N, Cook M, Dreyer M, Duclos O, Eubanks B, Fairbanks K, Finley S, Forknall N, Francis A, Hopkins GP, Joyce EM, Kim S, Kirk NA, Kovalyak J, Lauchie SA, Lohff A, Maldonado C, Manley EA, McLin S, Mooney C, Ndama M, Ogundeyi O, Okeoma N, Ordish C, Padilla N, Patrick C, Paterson T, Phillips EE, Phillips EM, Rampally N, Ribeiro C, Robertson MK, Rymer JT, Ryan SM, Sammons M, Scott AK, Scott AL, Shinomiya A, Smith C, Smith K, Smith NL, Sobeski MA, Suleiman A, Swift J, Takemura Satoko, Talebi I, Tarnogorska D, Tenshaw E, Tokhi T, Walsh JJ, Yang T, Horne JA, Li F, Parekh R, Rivlin PK, Jayaraman V, Ito K, Saalfeld S, George R, Meinertzhagen I, Rubin GM, Hess HF, Scheffer LK, Jain V, Plaza SM. 2020. A Connectome of the Adult Drosophila Central Brain. *bioRxiv* 2020.01.21.911859. doi:10.1101/2020.01.21.911859

Yagi R, Mabuchi Y, Mizunami M, Tanaka NK. 2016. Convergence of multimodal sensory pathways to the mushroom body calyx in Drosophila melanogaster. *Scientific Reports* **6**:1–8. doi:10.1038/srep29481

Yau JM, DeAngelis GC, Angelaki DE. 2015. Dissecting neural circuits for multisensory integration and crossmodal processing. *Philosophical Transactions of the Royal Society B: Biological Sciences* **370**:20140203. doi:10.1098/rstb.2014.0203

Zheng Z, Lauritzen JS, Perlman E, Robinson CG, Nichols M, Milkie D, Torrens O, Price J, Fisher CB, Sharifi N, Calle-Schuler SA, Kmecova L, Ali IJ, Karsh B, Trautman ET, Bogovic JA, Hanslovsky P, Jefferis GSXE, Kazhdan M, Khairy K, Saalfeld S, Fetter RD, Bock DD. 2018. A Complete Electron Microscopy Volume of the Brain of Adult Drosophila melanogaster. *Cell* **174**:730-743.e22. doi:10.1016/j.cell.2018.06.019

Table 1. Neurons projecting to the dorsal accessory calyx.

Name of neuron	Cluster	Line number	GRASP signal	Connectivity rate
$_{LO}$**PN1**	PLP cluster	R44H11	strong signal	4.1% (*n* = 27)
$_{LO}$**PN2**	PLP cluster	R72D07	strong signal	3.0% (*n* = 27)
$_{PLP}$**PNs (group)**	LH cluster	R19H07 and R20G07	strong signal	14.1% (*n* = 24)
$_{PLP}$**PN (single)**	LH cluster	R19H07 and R20G07	N/A	1.9% (*n* = 32)
$_{PAL}$**PN1**	AL cluster	R30E11 and R31C03	weak signal	0 (*n* = 26)
$_{PAL}$**PN2**	AL cluster	R53B06	weak signal	0 (*n* = 30)
$_{PAL}$**PN3**	AL cluster	R11F08 and R12C04	no signal	0 (*n* = 26)
$_{PAL}$**PN4**	AL cluster	R11F07	no signal	0 (*n* = 25)
$_{PAL}$**PN5**	AL cluster	R64G05	no signal	N/A
$_{ME}$**PN1**	OL cluster	R21B02	no signal	N/A

685

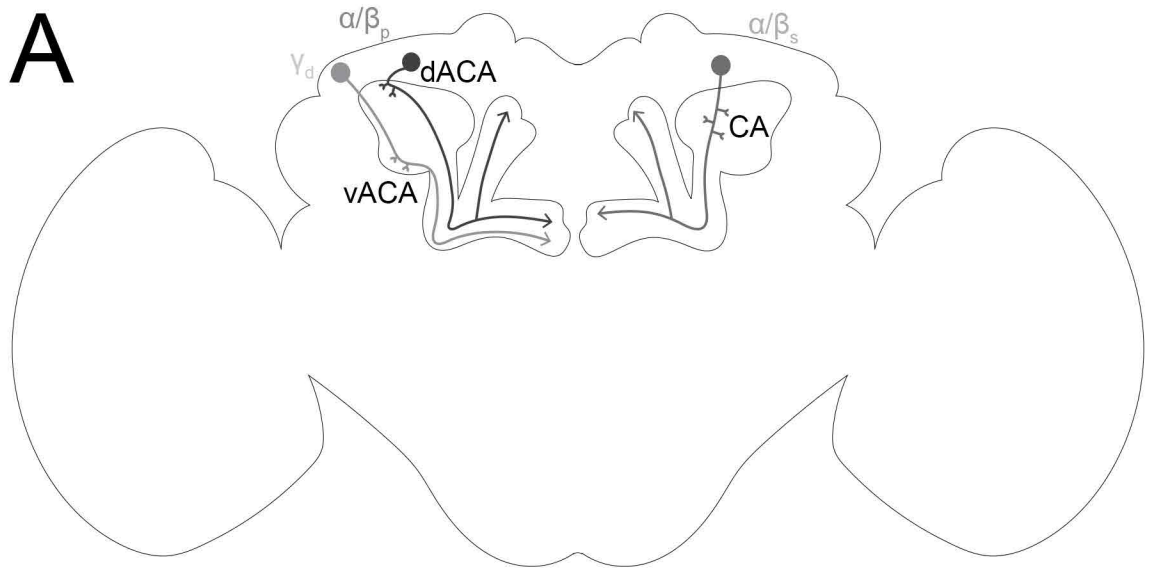

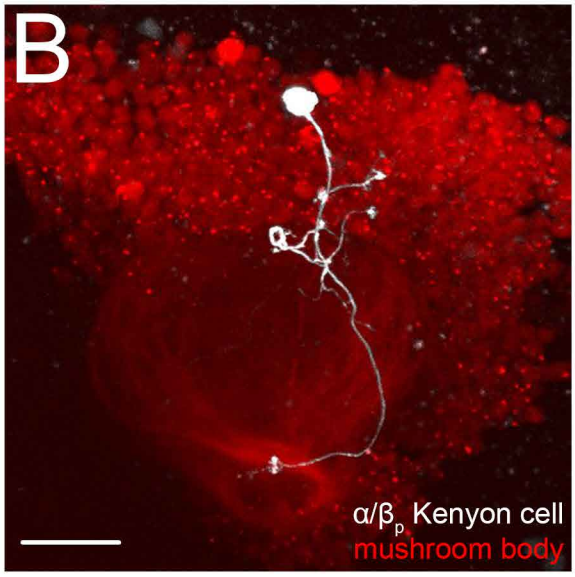

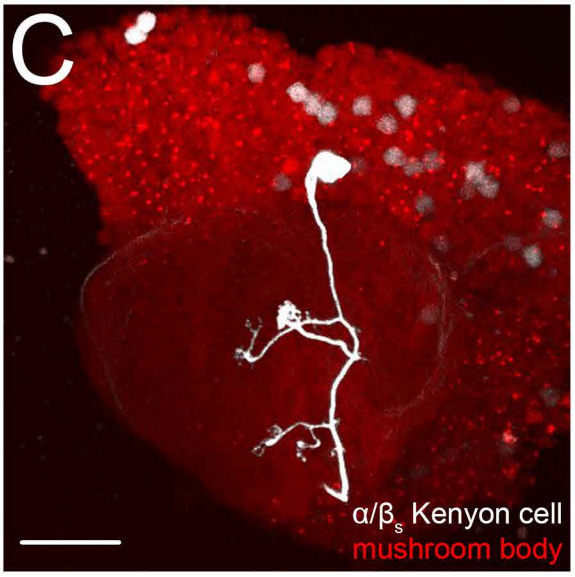

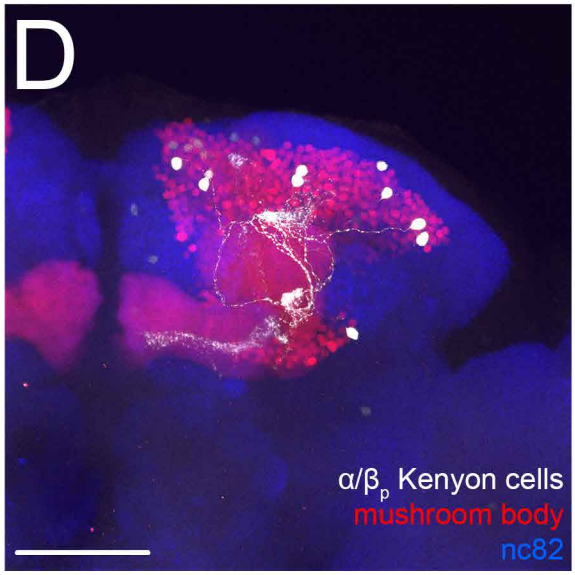

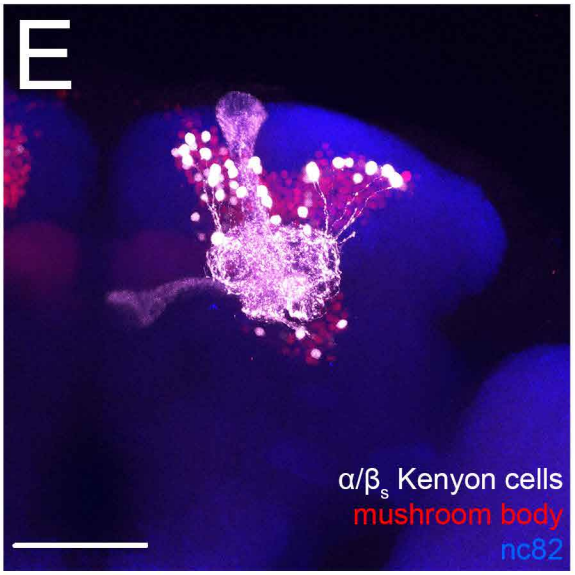

Figure 1. The dorsal accessory calyx of the *Drosophila melanogaster* mushroom body is formed by the α/β_p Kenyon cells. (A) A schematic of the *Drosophila* brain shows three types of Kenyon cell associated with the different mushroom body calyces: the α/β_p Kenyon cells (dark grey) extend their dendrites in the dorsal accessory calyx (dACA), the α/β_s (medium grey) — as well as the α'/β'_{ap}, α'/β'_m and γ_{main} Kenyon cells (not depicted) — extend their dendrites in the main calyx (CA) and the γ_d Kenyon cells (light grey) extend their dendrites in the ventral accessory calyx (vACA). (B) (B-C) A single α/β_p (B) or α/β_s (C) Kenyon cell (white) of the mushroom body (red) was photo-labeled. (D-E) Many α/β_p (D) or α/β_s (E) Kenyon cells (white) of the mushroom body (red) were photo-labeled; brains were fixed and stained using the anti-nc82 antibody (blue). The following genotypes were used in this figure: (B, D) *yw*/*yw*;*MB247-DsRed*^{unknown},*UAS-C3PA-GFP*^{unknown}/*UAS-SPA-GFP*^{attp40};*UAS-C3PA-GFP*^{attP2},*UAS-C3PA-GFP*^{VK00005},*UAS-C3PA-GFP*^{VK00027}/*R13F02-GAL4*$_{AD}^{VK00027}$,*R85D07-GAL4*$_{DBD}^{attP2}$; (C and E): *yw/yw*;*MB247-DsRed*^{unknown}*UAS-C3PA-GFP*^{unknown}/*R52H09-GAL4*$_{AD}^{attp40}$;*UAS-C3PA*^{attp2},*UAS-C3PA*^{VK00005},*UAS-C3PA*^{VK00027}/*R18F09-GAL4DBD*^{attp2}. Scale bars are 20 µm in (B-C) and 50 µm in (D-E).

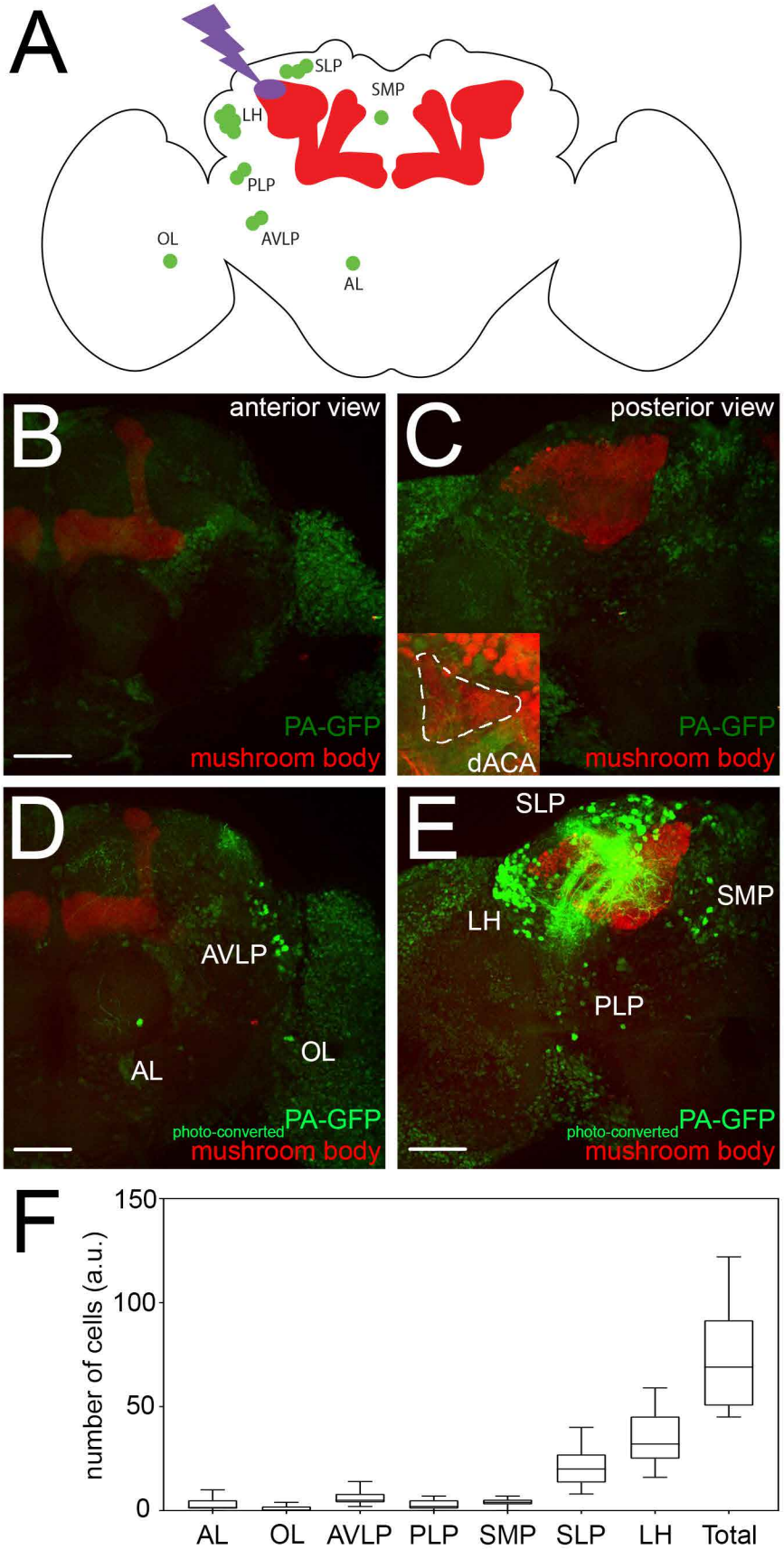

Figure 2. **Identification of neurons projecting to the dorsal accessory calyx using *en masse* photo-labeling.** (A) A schematic of the *Drosophila* brain shows the seven clusters of neurons identified by photo-labeling the dorsal accessory calyx of the mushroom body. (B-C) All neurons — expect for Kenyon cells (red) — express PA-GFP (green) showing weak fluorescence in structures located on the anterior (B) and posterior (C) sides of the brain. The dorsal accessory calyx (C, inset) was visible in the red channel and targeted for photo-labeling. (D-E) Upon photo-activation of PA-GFP in the dorsal accessory calyx, seven clusters of photo-labeled neurons are clearly distinguishable in different brain regions located on the anterior (D) and posterior (E) sides of the brain. (F) This procedure recovered a total of 71 neuronal cell bodies (71 ± 22, n = 22) in seven different clusters located near or in the antennal lobe (AL), optic lobe (OL), anterior ventral lateral protocerebrum (AVLP), lateral horn (LH), superior lateral protocerebrum (SLP), superior medial protocerebrum (SMP) and posterior lateral protocerebrum (PLP). The following genotype was used in this figure: *yw*/*yw*;*MB247-DsRed*^{unkown},*UAS-C3PA-GFP*^{unkown}/*MB247-GAL80*^{unkown}, *UAS-SPA-GFP*^{attp40};*UAS-C3PA-GFP*^{attp2},*UAS-C3PA*^{VK00005},*UAS-C3PA*^{VK00027}/*N-Synaptobrevin-GAL4*$^{2-1}$. Scale bars are 50 µm in all panels.

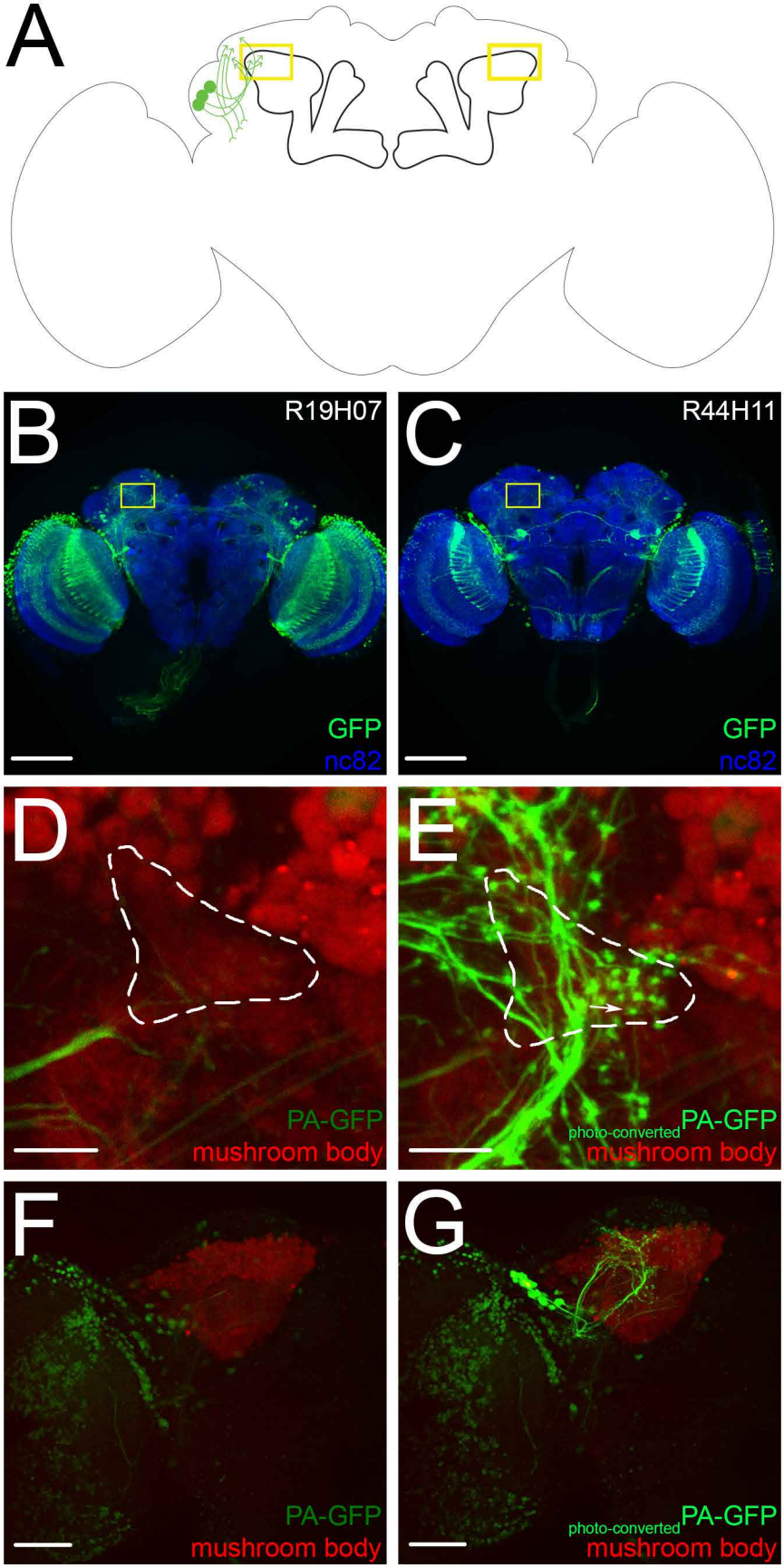

Figure 3. Anatomical screen to identify transgenic lines driving expression in the neurons projecting to the dorsal accessory calyx. (A) A schematic of the *Drosophila* brain shows the region of interest (yellow rectangle) used to screen the FlyLight database for potential dorsal accessory calyx input neurons. (B-C) First, the expression patterns of each of the transgenic lines available in this database was screened: transgenic lines clearly driving expression in neurons projecting to or from the dorsal accessory calyx were selected for further investigation (B: *R19H07-GAL4* and C: *R44H11-GAL4*). (D-E) The dorsal accessory calyx (white dotted line) of the mushroom body (red) was visualized in the selected lines and targeted for photo-labeling, revealing potential input neurons. (F-G) Transgenic lines driving expression in a few neurons extending clear axonal terminals in the dorsal accessory calyx (arrow) were selected for further investigation. Before photo-labeling, weak fluorescence is visible in many different neurons (B,D) but, upon photo-labeling, only the neurons projecting to the dorsal accessory calyx are visible (C, E). The following genotype was used in this figure: *yw*/*yw*;*MB247-DsRed*^{unknown},*UAS-C3PA-GFP*^{unknown}/*UAS-C3PA-GFP*^{attP40};*UAS-C3PA*^{attP2},*UAS-C3PA*^{VK00005},*UAS-C3PA*^{VK00027}/*R19H07-GAL4*^{attP2}. Scale bars are 100 µm (B-C), 10 µm (D-E) and 50 µm (F-G).

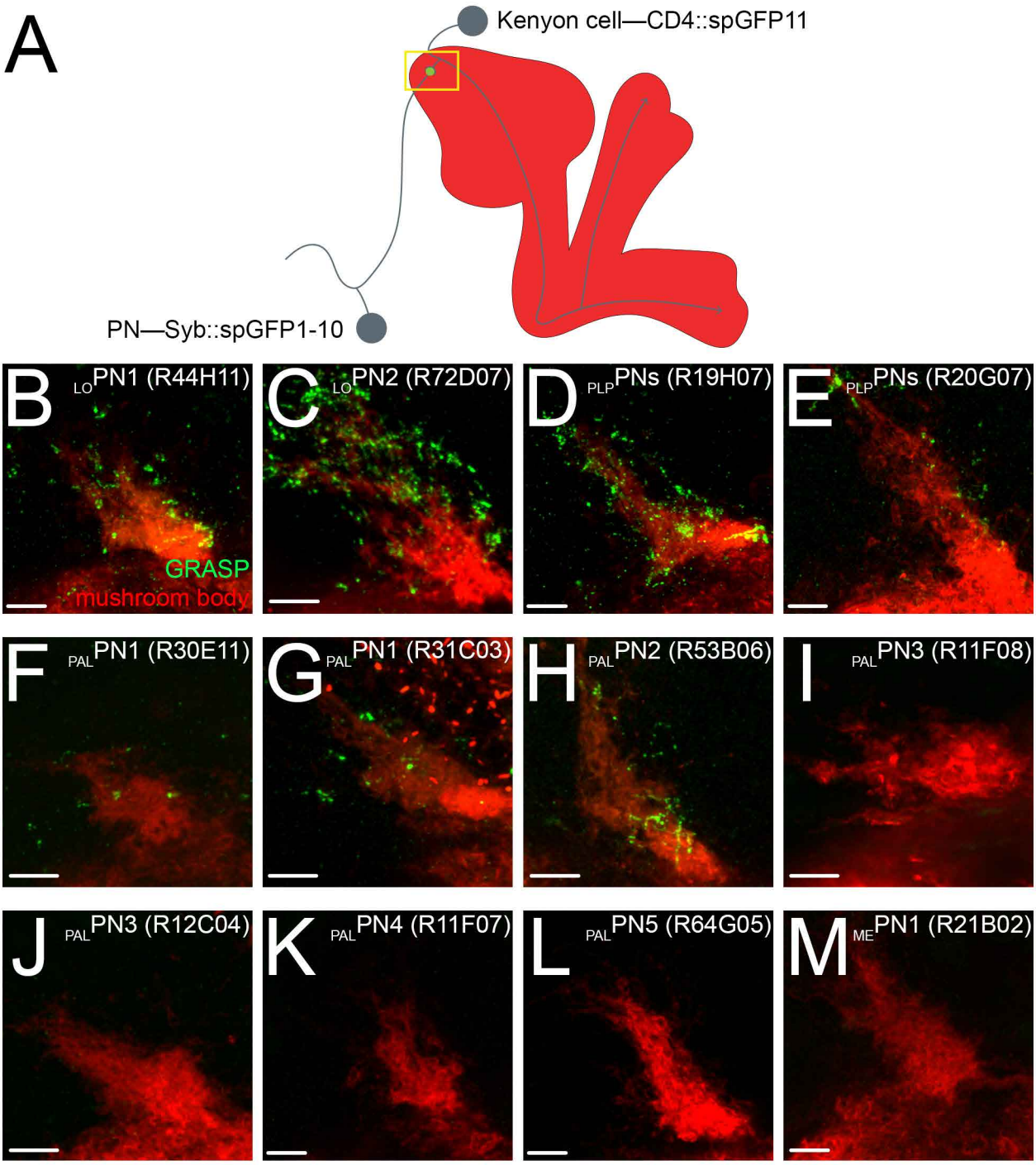

Figure 4. Identification of the transgenic lines driving expression in neurons presynaptic to the α/β_p Kenyon cells. (A) A schematic of the *Drosophila* brain shows how the GFP Reconstitution Across Synaptic Partners (GRASP) technique was used to identify the transgenic lines that drive expression in neurons presynaptic to the α/β_p Kenyon cells. The expression of the spGFP1-10 fragment was driven in the putative input neurons (here $_{PLP}$PNs, pink) using the transgenic lines identified in the screen and the expression of the spGFP11 fragment was driven in most Kenyon cells (red). Reconstituted GFP molecules (green) are visible in the dorsal accessory calyx of the mushroom body (red) when the spGFP$^{1-10}$ fragment is expressed in a α/β_p Kenyon cell synaptic partner. (B-M) A strong (B-E) or weak (F-H) GRASP signal was detected using some transgenic lines; no GRASP signal was detected using other lines (I-M). The following genotypes were used in this figure: *yw*/*yw*;*UAS-syb::spGFP1-10*^{unknown}, *LEXAop-CD4::spGFP11*^{unknown}/*LEXAop-tdTomato*^{attP5};*R_line-GAL4*^{attP2}(as indicated on the panel)/*MB247-LEXA*^{unkown}. Scale bars are 5 µm in all panels.

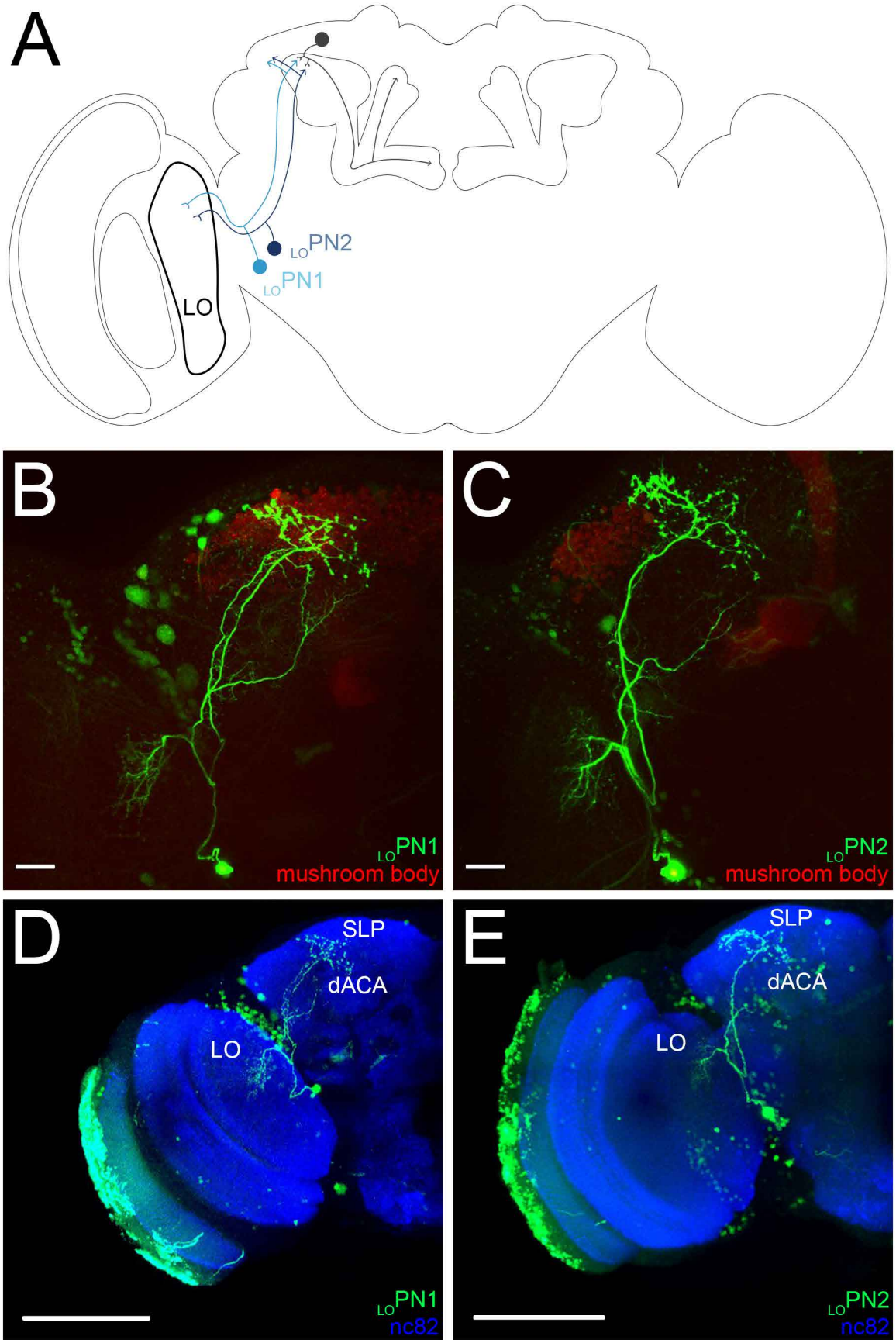

Figure 5. $_{LO}$PNs connect the lobula to the dorsal accessory calyx. (A) A schematic of the *Drosophila* brain shows two α/β_p Kenyon cell input neurons — $_{LO}$PN1 (light blue) and $_{LO}$PN2 (dark blue) — projecting from the lobula. (B-C) $_{LO}$PNs — $_{LO}$PN1 (B, bright green) and $_{LO}$PN2 (C, bright green) — were recovered from the screen and show overall similar morphology. (D-G) $_{LO}$PNs — $_{LO}$PN1 (D,F; bright green) and $_{LO}$PN2 (E,G; bright green) — were photo-labeled, fixed and stained using the anti-nc82 antibody (blue). Both neurons show overall similar but different innervation patterns: their somata are located near the optic lobe (D-G); they extend axonal terminals in the dorsal accessory calyx (dACA) and the superior lateral protocerebrum (SLP) (D-E); and they innervate a small region of the lobula (LO) (F-G). The following genotypes were used in this figure: (B, D, F) *yw*/*yw*;*MB247-DsRed*^{unknown},*UAS-C3PA-GFP*^{unknown}/*UAS-C3PA-GFP*^{attP40};*UAS-C3PA-GFP*^{attP2},*UAS-C3PA-GFP*^{VK00005},*UAS-C3PA-GFP*^{VK00027}/*R44H11-GAL4*^{attP2} and (C, E, G) *yw*/*yw*;*MB247-DsRed*^{unknown},*UAS-C3PA-GFP*^{attP40}/*UAS-C3PA-GFP*^{unknown};*UAS-C3PA-GFP*^{attP2},*UAS-C3PA-GFP*^{VK00005},*UAS-C3PA-GFP*^{VK00027}/*R72D07-GAL4-GFP*^{attP2}. Scale bars are 100 µm (D-E) and 20 µm (B,C,F,G).

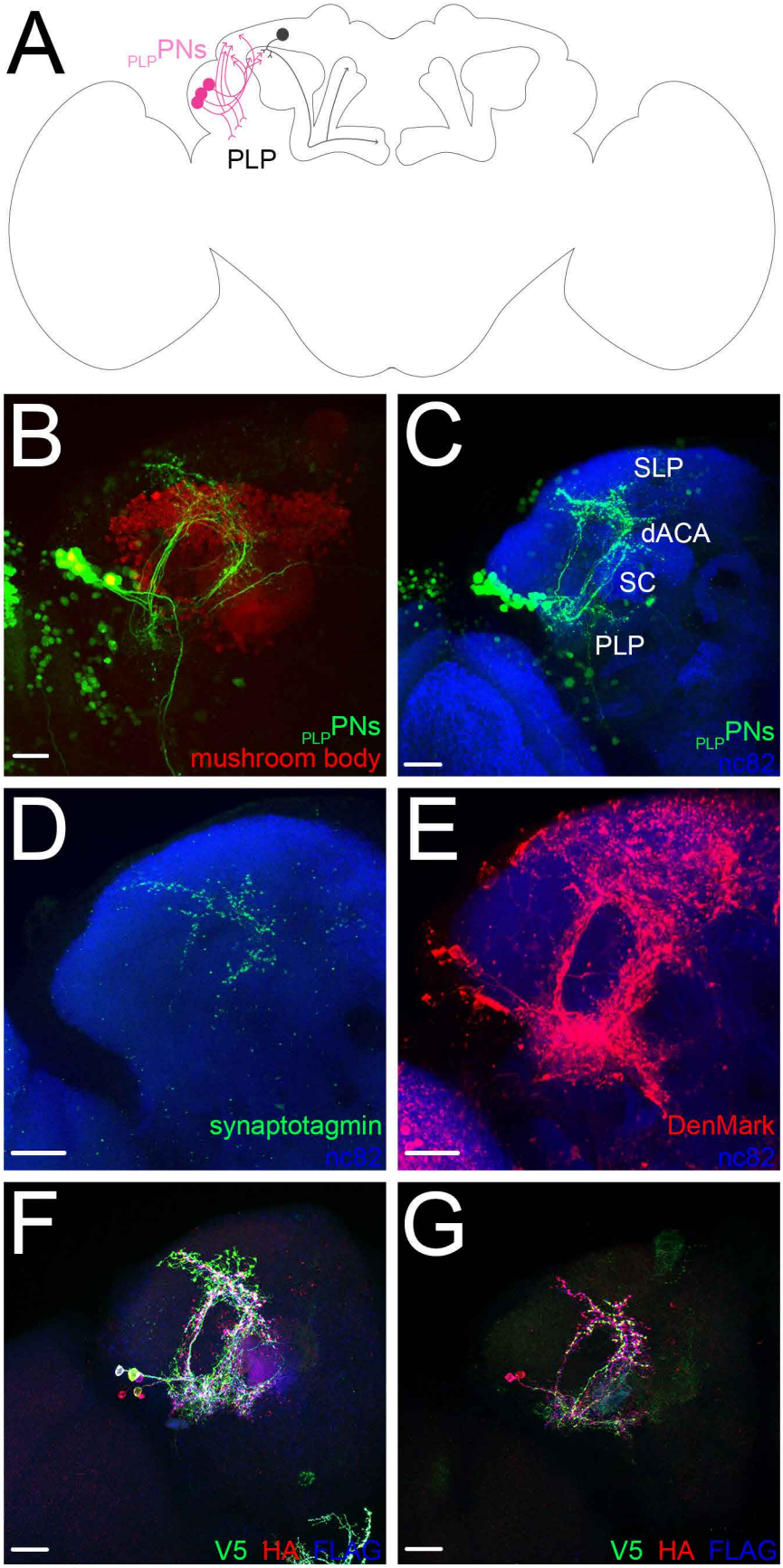

Figure 6. $_{PLP}$PNs connect the posterior lateral protocerebrum to the dorsal accessory calyx.

(A) A schematic of the *Drosophila* brain shows the α/β_p Kenyon cell input neuron, $_{PLP}$PN (pink), projecting from the posterior lateral protocerebrum. (B) A group of $_{PLP}$PNs (bright green) were recovered from the screen. (C) $_{PLP}$PNs were photo-labeled, fixed and stained using the anti-nc82 antibody (blue). All $_{PLP}$PNs show an overall similar innervation pattern: their somata are located near the lateral horn and they extend projections in the posterior lateral protocerebrum (PLP), the superior clamp, the superior lateral protocerebrum and the dorsal accessory calyx. (D-G) A split GAL4 transgenic line driving expression specifically in the $_{PLP}$PNs was engineered and used to drive the expression of the presynaptic marker synaptotagmin-fused GFP (D), the post-synaptic maker DenMark (E) or the MultiColor FlpOut transgenes (F-G). (F,G) Each $_{PLP}$PN expresses a stochastic combination of three epitopes (V5, HA and/or FLAG), giving each neuron a different color upon antibody staining. The overall morphology of individual $_{PLP}$PNs are similar, with slightly different neurite branching patterns. The following genotypes were used in this figure: (B-C) *yw*/*yw*; *MB247-DsRed*^{unknown}, *UAS-C3PA-GFP*^{unknown}/*UAS-C3PA-GFP*^{attP40};*UAS-C3PA-GFP*^{attP2}, *UAS-C3PA-GFP*^{VK00005},*UAS-C3PA-GFP*^{VK00027}/*R19H07-GAL4*^{attP2}; (D) *yw*/*yw*;*Sp*/*CyO*; *R20G07-GAL4*$_{DBD}$^{attP2},*R19H07-GAL4*$_{AD}$^{VK00027}/*UAS-synaptotagmin::GFP*^{unknown}; (E) *yw*/*yw*;*UAS-DenMark*^{2}/*CyO*; *R20G07-GAL4*$_{DBD}$^{attP2},*R19H07-GAL4*$_{AD}$^{VK00027}/*Tm2*; and (F-G) *yw*/*yw*;*Sp*/*CyO*; *R20G07-GAL4*$_{DBD}$^{attp2},*R19H07-GAL4*$_{AD}$^{VK00027}/*UAS-FRT>STOP>FRT-myr::smGdP-HA*^{VK00005}, *UAS-FRT>STOP>FRT-myr::smGdP-V5-THS,UAS-FRT>STOP>FRT-myr::smGdP-FLAG*$^{su(Hw)attP1}$. Scale bars are 20 μm in all panels.

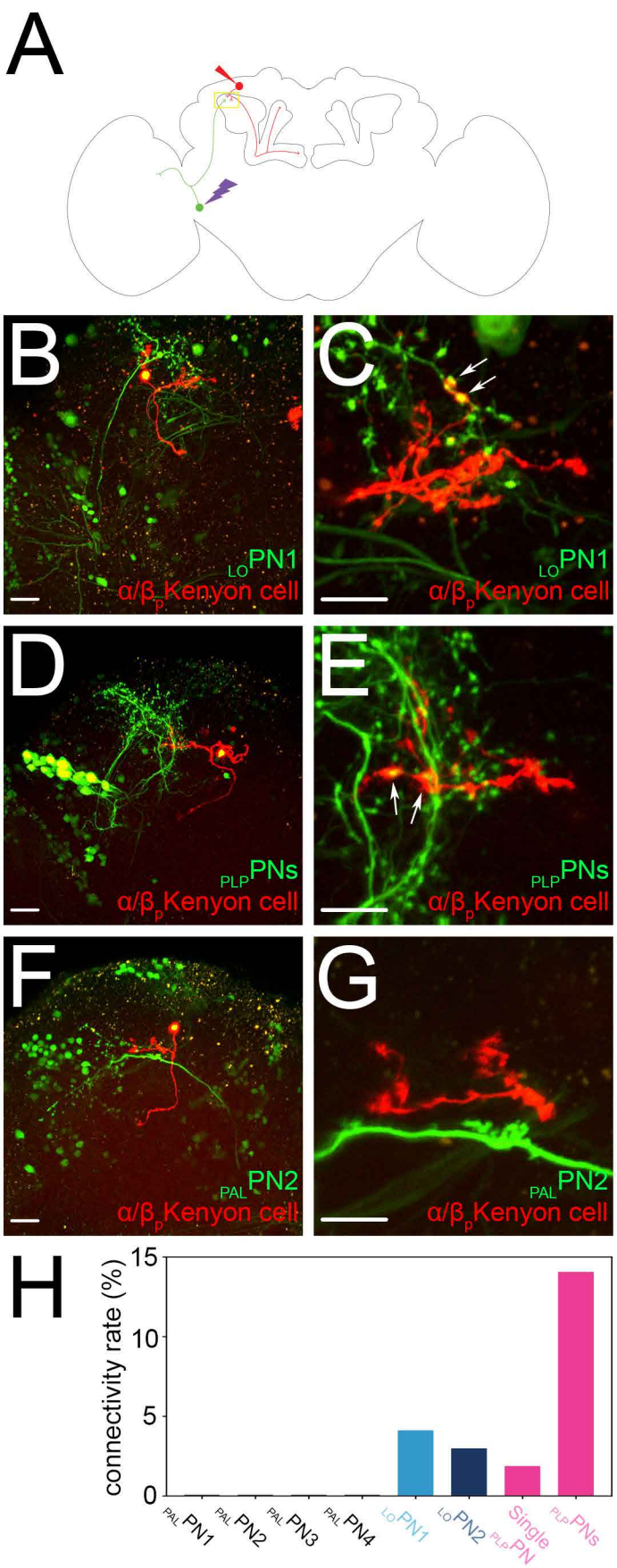

Figure 7. Frequency of connections between the α/β$_p$ Kenyon cells and their input neurons. (A) A schematic of the *Drosophila* brain shows how the frequency of connections between the α/β$_p$ Kenyon cells (red) and $_{LO}$PN1 (green) was measured. (B-G) A given input neuron was photo-labeled (green) and a randomly chosen α/β$_p$ Kenyon cell was dye-filled (red). The total number of claws formed by the dye-filled Kenyon cell was counted and claws connecting to the axonal terminals of the photo-labeled neuron were detected (arrows). Such connections were found for $_{LO}$PN1 (B-C), $_{LO}$PN2 and $_{PLP}$PNs (D-E) but not for the other neurons identified in this study such as $_{PAL}$PN2 (F-G). (H) The frequency of connections between α/β$_p$ Kenyon cells and a given projection neuron was calculated by dividing the number of connections detected (for instance arrows in C and E) by the total number of claws sampled for that particular projection neuron. The following genotypes were used in this figure: *yw*/*yw*;*UAS-C3PA-GFP*^{unknown}/*UAS-SPA-GFP*^{attP40}; *R13F02-GAL4*$_{AD}^{VK00027}$,*R85D07-GAL4*$_{DBD}^{attP2}$/*R_line*(as indicated in the panel)-*GAL4*^{attP2}. Scale bars are 20 μm (B, D, F) and 10 μm (C, E, G).

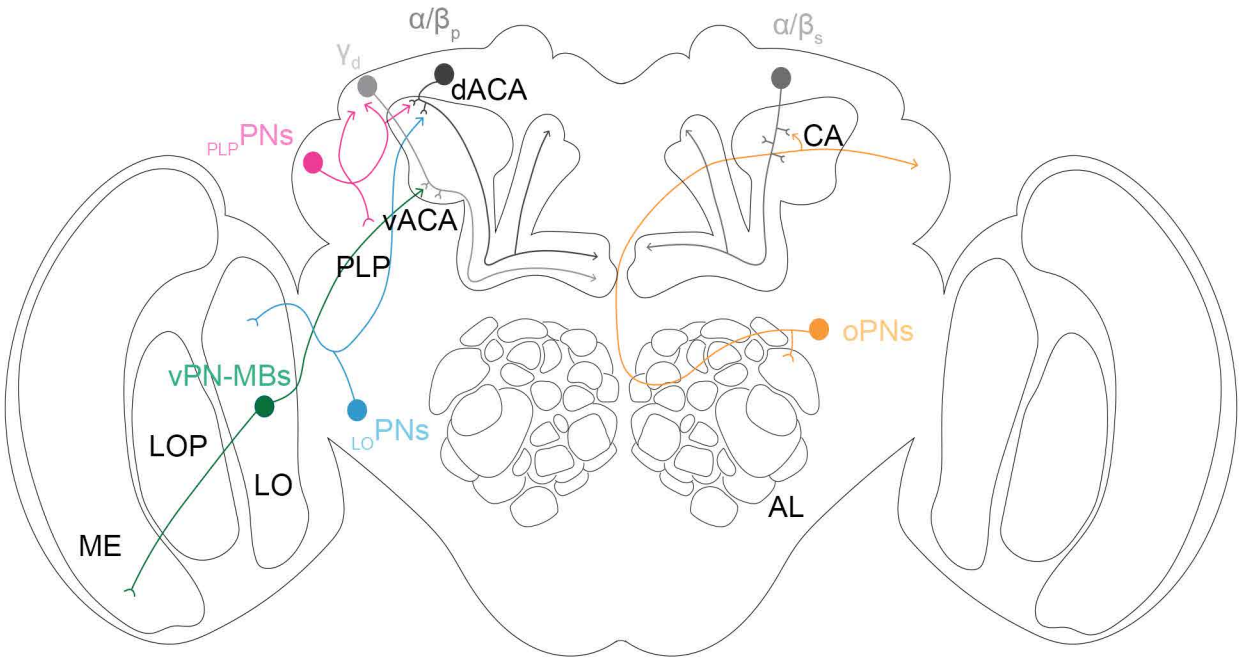

Figure 8. Visual information is conveyed to the mushroom body through two parallel pathways. The main calyx (CA) of the mushroom body receives input from the olfactory system: neurons projecting from the antennal lobe (orange) form synapses with the Kenyon cells associated with the main calyx, such as the α/β_s Kenyon cells. The dorsal accessory calyx (dACA) and the ventral accessory calyx (vACA) receive input from the visual system: neurons projecting from the lobula ($_{LO}$PNs, blue) form synapses with the α/β_p Kenyon cells associated with the dorsal accessory calyx, whereas neurons projecting from the medulla ($_{ME}$PNs, green) form synapses with the γ_d Kenyon cells associated with the ventral accessory calyx. The dorsal accessory calyx also receives input from the posterior lateral protocerebrum via the $_{PLP}$PNs (pink).